ELSEVIER

Colloids and Surfaces A: Physicochem. Eng. Aspects 254 (2005) 81–89

COLLOIDS AND SURFACES A

www.elsevier.com/locate/colsurfa

Electrocoagulation for removal of silica nano-particles from chemical–mechanical-planarization wastewater

Walter Den[a,*], Chihpin Huang[b,1]

[a] *Department of Environmental Science, Tunghai University, Taichung-Kan Road, Sec. 3, #181, P.O. Box 818, 407 Taichung, Taiwan, Republic of China*
[b] *Institute of Environmental Engineering, National Chiao Tung University, Po-Ai St., #75300 Hsinchu, Taiwan, Republic of China*

Received 16 April 2004; accepted 26 November 2004
Available online 30 December 2004

Abstract

Continuous-flow electrocoagulation process with vertical flow-channels was investigated as a method to treat synthetic chemical–mechanical-planarization (CMP) wastewater containing highly charged ultrafine silica particles ($\zeta = -55$ mV, mean $R_p = 45$ nm at pH 9.5). The parallel-plate, monopolar electrochemical cells resembled a series of closed electrical circuits such that the electrical field strength was highly dependent of the current density and aqueous conductivity, but independent of the inter-electrode gap. The residual turbidity of the CMP wastewater decreased with the increases in either hydraulic retention time or applied current density, and removal efficiency as high as 95% was achieved for wastewater with both low (70 NTU) and high (400 NTU) initial turbidities. The charge loading linearly correlated with turbidity removal efficiency up to a level of 8 F m^{-3}, presenting an appropriate design parameter. Further analysis indicated that turbidity removal was limited by the quantity of liberated ferrous ions at lower range of current density, but seemingly reached a critical level of current density beyond which the process performance gradually deteriorated. Comparisons between the effective particle retention time and the estimated electrophoretic migration time revealed that the electrocoagulation process was predominantly controlled by the rate of particle aggregation occurring near the anodic surfaces. Furthermore, this process generates lesser amount of dry sludge as compared to chemical coagulation with polyaluminum chloride, and does not require pH adjustment prior to treatment.

Keywords: Electrocoagulation; Electrochemical; Parallel plate; Monopolar; Silica colloids; Chemical–mechanical-planarization; CMP wastewater treatment

1. Introduction

Chemical–mechanical-planarization (CMP) is one of the fastest growing processes in semiconductor manufacturing, and has become an integral part of the state-of-the-art fabrication line for the multi-level design of integrated circuit (IC). The process is primarily used for "polishing" the device side of a semiconductor wafer through the mechanical downforce of slurry abrasive in combination with the chemical oxidation of wafer surface. Due to its capability to achieve uniform surface topography with high throughput, the use of CMP technology has expanded from the traditional application in metal interconnects (i.e., metal CMP) to more complicated applications in dielectric barrier layer planarization (i.e., oxide CMP). With the continuing pursuit of functionally stronger devices with smaller feature sizes (sub 0.25 μm), the device fabrication will undoubtedly rely more and more on the CMP processes [1]. As a consequence, the quantity of CMP wastewater generated is expected to increase proportionally with the growing needs of the CMP processes [2]. Furthermore, as the International Technology Roadmap for Semiconductors [3] specifies, the objective of reducing total water consumption by roughly five-fold for fabrication processes must be met by 2005, with more than 80% water recycling capability for the new plants. This industry-wide effort of water conservation and recycling translates to higher solid

* Corresponding author. Tel.: +886 4 23590121x3050; fax: +886 23594276.
E-mail addresses: wden@mail.thu.edu.tw (W. Den), cphuang@mail.nctu.edu.tw (C. Huang).
[1] Tel.: +886 3 5726463; fax: +886 5725958.

0927-7757/$ – see front matter © 2004 Elsevier B.V. All rights reserved.
doi:10.1016/j.colsurfa.2004.11.026

Nomenclature

A_p	effective area of anode (m^2)
E	electrical field strength ($V\,m^{-1}$)
E_{eq}	equilibrium potential difference between electrodes (V)
F	Faraday constant (96,500 C)
i	applied current (A)
j	current density ($A\,m^{-2}$)
l_p	inter-electrode distance (m)
N	number of anodic plates
q	particle charge (C)
R_p	mean particle radius (m)
T_0, T	initial and variable wastewater turbidity (NTU)
u	electrophoretic migration velocity ($m\,s^{-1}$)
V_r	working volume of wastewater in reactor (m^3)

Greek letter

ε	dielectric constant
η	over-potential (V)
κ	aqueous conductivity ($mho\,m^{-1}$)
μ	dynamic viscosity of water ($kg\,m^{-1}\,s^{-1}$)
τ	hydraulic retention time (min)
ζ	zeta potential (V)

concentration in CMP wastewater, which must be properly treated to meet the local discharge regulations.

CMP effluents typically contain suspended solids originated from slurry abrasive particles of SiO_2, Al_2O_3, or CeO_2, depending on the nature of the CMP application. Other contaminants, including insoluble metal oxides and nitrides and soluble chemicals, also exist in the wastewater in a much lesser quantity. Golden et al. [4,5] have described the chemistry of CMP wastewater in detail. In principal, CMP wastewater contains very dilute slurry abrasives that are narrowly ranged between 50 and 200 nm, and possess highly negative surface charges that repel adjacent particles when they are immersed in base solutions. These wastewater characteristics render conventional coagulation–flocculation technology less ideal to remove such nano-scale particles from the CMP wastewater. A common problem experienced by many system operators is the need to increase the coagulant dosage, leading to bulky sludge volume. Additionally, the poor settling characteristics of the flocs often prolong the settling time to achieve the necessary separation efficiency. To overcome these problems, membrane separation process has been adapted as a single unit or as a post separator for coagulation/flocculation process [6–9]. The use of membrane filtration has demonstrated success in the removal of suspended solids, and owns the added value of re-concentrate the valuable slurry for possible reuse. However, maintaining the necessary degree of permeate flux is still an issue of concern.

As an alternative treatment method, electrochemical processes have been proposed and investigated to treat wastewater containing dispersed ultra-fine particles without chemical additions [10–14]. Belongia et al. [10] first demonstrated that, when passing an electrical current through CMP suspensions, two distinct solid separation phenomena, namely electrodecantation and electrocoagulation, occurred. The occurrence of these phenomena strongly depends on the type of slurry and the conductivity of the suspension. For electrocoagulation, the sacrificial anodic electrodes of iron and aluminum are commonly used to continuously supply metallic ions as the source of coagulants. These electrochemically generated metallic ions can hydrolyze near the anode to form a series of metallic hydroxides capable of destabilizing dispersed particles. The simultaneous electrophoretic migration of the negatively charged particles (e.g., silica particles) toward the anode forces chemical coagulation between particles and metallic hydroxides in the vicinity of the anode, forming flocs that either settles or re-deposits onto the anode (Fig. 1). Matteson et al. [13] developed a mathematical model based on electrophoresis and charge neutralization to simulate the kinetics of electrocoagulation process for ultra-fine kaolin particles. They found that a second-order reaction kinetics could be used to generically describe the particle aggregation and removal processes. Den et al. [14] have also demonstrated efficient particle separation by electrocoagulation of dispersed silica particles in a continuous-flow mode, although the roles of particle transport and reaction were not clarified. Therefore, the primary objective of the present work was to investigate the effects of major parameters, including transport and electrochemical parameters, in the design and operation of the continuous-flow electrocoagulation reactor for treatment of oxide CMP wastewater consisting primarily of nano-size silica.

2. Materials and methods

2.1. CMP wastewater preparation

Silica suspensions were prepared by diluting a commercially available, KOH-based CMP slurry containing 25 wt.% fume silica (Semi-Sperse® 25 slurry, Cabot Microelectronics Corp., USA). The original slurry was diluted to 0.05% and 0.4% with deionized water, yielding suspension turbidity of approximately 70 and 400 NTU, respectively. These slurry dilution levels correspond to particle number concentrations of 4.55×10^{17} and $3.65 \times 10^{18}\ m^{-3}$ for a nominal silica density of $2.1\ g\,cm^{-3}$ and particle size of 0.1 μm. Table 1 presents the physical and chemical properties of several oxide CMP wastewater from different chip manufacturing facilities, as well as those of the synthetic wastewater used in this study. The oxide CMP wastewater primarily consists of dilute silica slurry with turbidity ranging between 100 and 350 NTU, pH between 8 and 9.5, conductivity between 100 and 140 $\mu S\,cm^{-1}$, and zeta potential between −50 and

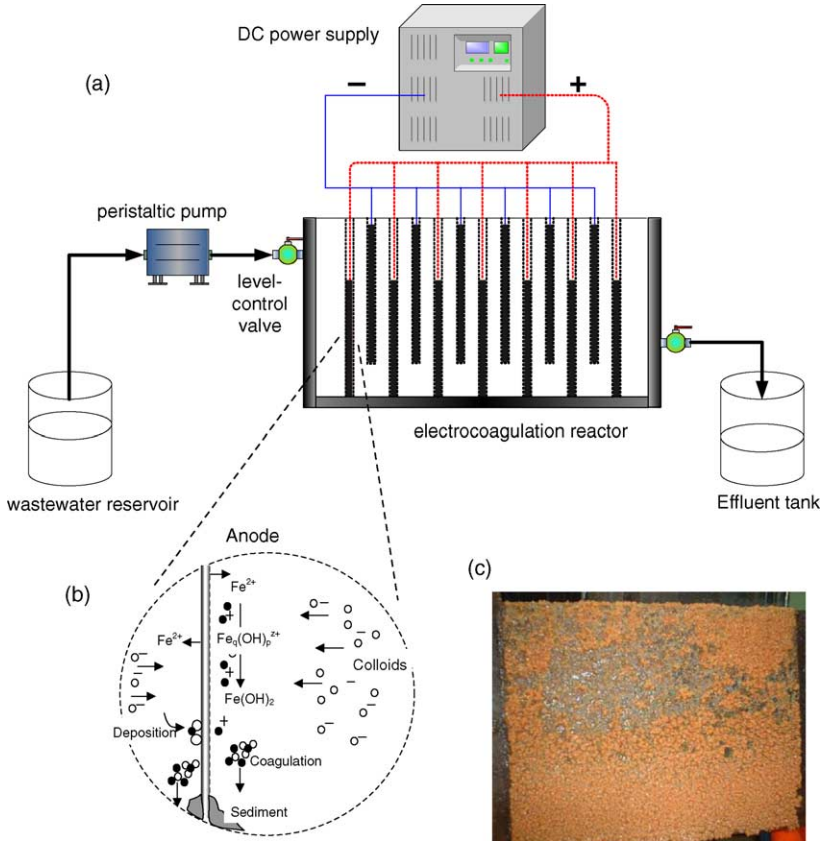

Fig. 1. (a) Experimental apparatus of continuous-flow electrocoagulation system. The magnified portion (b) schematically depicts the electrocoagulation mechanisms for the removal of colloidal particles, with the image (c) of the anode surface covered with gelatinous film.

−80 mV. In this study, the silica CMP suspension was maintained in a weak alkaline condition (pH ∼9.5) by 0.01 M KOH for the purpose of maintaining particle dispersion and softening the surface of silica particle by hydrolysis of Si–O–Si bonding:

$$\text{Si–O–Si} + \text{H}_2\text{O} \leftrightarrow \text{Si–OH} \quad (1)$$

$$\text{Si–OH} + \text{OH} \leftrightarrow \text{Si–O}^- + \text{OH : H} \quad (2)$$

The silica particles submerged in base solutions tend to adsorb OH^- on particle surface and form $Si–O^-$ on the surface extension. Therefore, increasing the OH^- concentration leads to greater degree of negative surface potential.

The particle size and distribution were measured by a particle analyzer (Honeywell UPA-150, Microtrac Inc., Montgomeryville, PA) using dynamic light scattering with an effective range between 0.001 and 6 μm. The electrophoretic mobility of the particles was measured by a zeta potential analyzer (ZetaPlus, Brookhaven Instruments Corp., Holtsville, NY) using Doppler shift analysis with laser light scattering. All samples were measured in duplicate to ensure data reproducibility, and an additional measurement was performed if necessary.

Table 1
Wastewater properties of the actual and synthetic oxide CMP effluent

Sample source	Mean particle size (nm)	Discharge ζ-potential (mV)	Discharge pH	Turbidity (NTU)	Total organic carbon (mg L^{-1})	Discharge conductivity (μS cm^{-1})
Source 1	165	−63.4	8–9	200–350	35–50	100
Source 2	170	−47.6	8.7–9.4	100–140	1.5–3.0	104–138
Source 3	>100[a]	−78.23	8.57	135	15.16	127.2
Synthetic wastewater (this study)	88	−55	9.3–9.7	70–400	0.5–10	55–150

Source 1: actual oxide CMP wastewater from a DRAM fabrication (Hsinchu, Taiwan).
Source 2: actual oxide CMP wastewater from a DRAM fabrication (Hsinchu, Taiwan) [7].
Source 3: wafer fabrication from Southern Taiwan [9].
[a] Estimated particle size for 90% weight distribution.

2.2. Monopolar electrocoagulation experiments

An 8-L continuous-flow reactor channelized by the electrode plates (20 cm × 14 cm) was designed and fabricated with clear acrylic to perform the experiments. As shown in Fig. 1a, alternate electrodes were connected to the opposite terminal power supply to form a monopolar configuration, giving a number of reactor cells electrically in parallel with one another. The anodes (iron plates) were completely submerged, and the cathodes (stainless steel plates) were partially submerged in the suspension. The channel width can be varied by adding or removing an equal number of electrode plates. The outlet port was located rather close to the bottom to prevent floating flocs from exiting the reactor. Electrical current was provided by a manually controllable dc power supply (Model GPS, Goodwill Instruments, Taiwan) operating in constant-current mode (range: 0–3 A). The voltage response (range: 0–200 V) was monitored and recorded by a data-acquisition system.

At the commencement of each experiment, the reactor was filled with CMP suspension such that the liquid level was approximately 1 cm above the anodic plates and below the top of the cathodic plates. The synthetic wastewater was continuously pumped from a 100-L reservoir into the reactor using a microprocessor-controlled peristaltic pump (Masterflex L/S, Cole Parmer, IL) at various flow rates between 80 and 380 mL min^{-1}, corresponding to mean hydraulic retention times between 20 and 100 min. Hence, an overall charge loading can be calculated using the following expression:

$$\text{charge loading}\,(C_F) = \frac{i\tau}{FV_r} \tag{3}$$

where i is the applied current (ampere), τ the mean hydraulic retention time (s), F the Faraday constant (96,500 C), and V_r the working volume (m^3) of the wastewater in the tank. During operation, a ball valve installed at the effluent end allowed control of steady liquid level in the reactor. Samples from the influent and effluent ports were taken at a 5-min interval and measured for turbidity, conductivity, and pH by a Hach ratio^{TM}/XR turbidity meter (Hach Co., Loveland, CO). The organic content in the suspensions was measured by a non-dispersive infrared TOC analyzer (Shimadzu TOC-5000A, Japan) after samples were filtered with 0.45-μm membrane, acidified, and N_2 purged to remove inorganic carbon. At the end of each experimental run, the total residual iron concentration was analyzed by inductively-coupled plasma-atomic emission spectroscopy (ICP-AES, Jobin-Yzon JY24, France).

2.3. Chemical coagulation experiments

Jar tests (PB-700 Jar tester, Phipps & Bird Inc., USA) were also performed on the synthetic CMP wastewater as a comparative basis between electro and chemical coagulation processes. Polyaluminum chloride (PACl) was chosen as the chemical coagulant. The stock PACl solution of 0.1 wt.% was freshly prepared by dissolving the reagent-grade PACl (Showa Chemicals Inc., Japan) in the deionized water. The alkalinity was adjusted to 100 mg L^{-1} (as $CaCO_3$) by adding $NaHCO_3$. The mixing conditions were provided with 1-min rapid mixing (200 rpm, $G = 350\ s^{-1}$), followed by 20-min slow mixing (30 rpm, $G = 25\ s^{-1}$). Sedimentation was allowed to occur for 40 min, and the residual turbidity of the supernatant was measured. These coagulation and mixing conditions were similar to those used to successfully treat clay suspensions as described elsewhere [15]. All coagulant dosages reported in this paper were in the unit of mg L^{-1} as Al.

3. Results and discussion

3.1. Characterization of synthetic CMP wastewater

Fig. 2a shows the surface potential (i.e., ζ-potential) of the diluted silica slurry and the corresponding particle size as a function of solution pH. The isoelectric point (IEP) for the suspension was 2.3, resulting in a mean particle size of approximately 130 nm. Under the weak alkaline condition (pH between 9 and 10) into which the wastewater discharged from the oxide CMP process typically falls, the dispersed particle formed a logarithmically normal distribution with a geometric mean particle size of 90 nm and a standard deviation of 1.42. Furthermore, the turbidity of the silica suspension exhibited a linear relationship with the slurry dilution levels for slurry concentration less than 1 wt.%, as shown in Fig. 2b. The typical range of turbidity of CMP wastewater was 50–500 NTU, which is equivalent to a dilution level of 50–200 times from the original slurry. The conductivity of the solution also increased linearly with the increasing slurry concentration (or turbidity) due to the presence of oxidizers or additives (e.g., KOH, NH_4OH) in the raw slurry. The range of these values is conformed to those reported for the actual oxide CMP wastewater (see Table 1), and thus justified the appropriateness of using the synthetic CMP wastewater as the model wastewater. The solution conductivity was not altered by any external ionic addition throughout the study of the electrocoagulation process.

3.2. Reactor analysis

The monopolar arrangement of anodes and cathodes connected in parallel to the dc power supply created multiple cells, each could be viewed as a closed electrical circuit having identical electrical potential, provided that the wastewater conductivity was sufficiently low to prevent “leaks” from the circuit. Theoretically, The required voltage for each electrochemical cell should include the equilibrium potential difference between the anode and cathode (E_{eq}), the over-potentials (η) due to anodic/cathodic mass transfer and charge-transfer

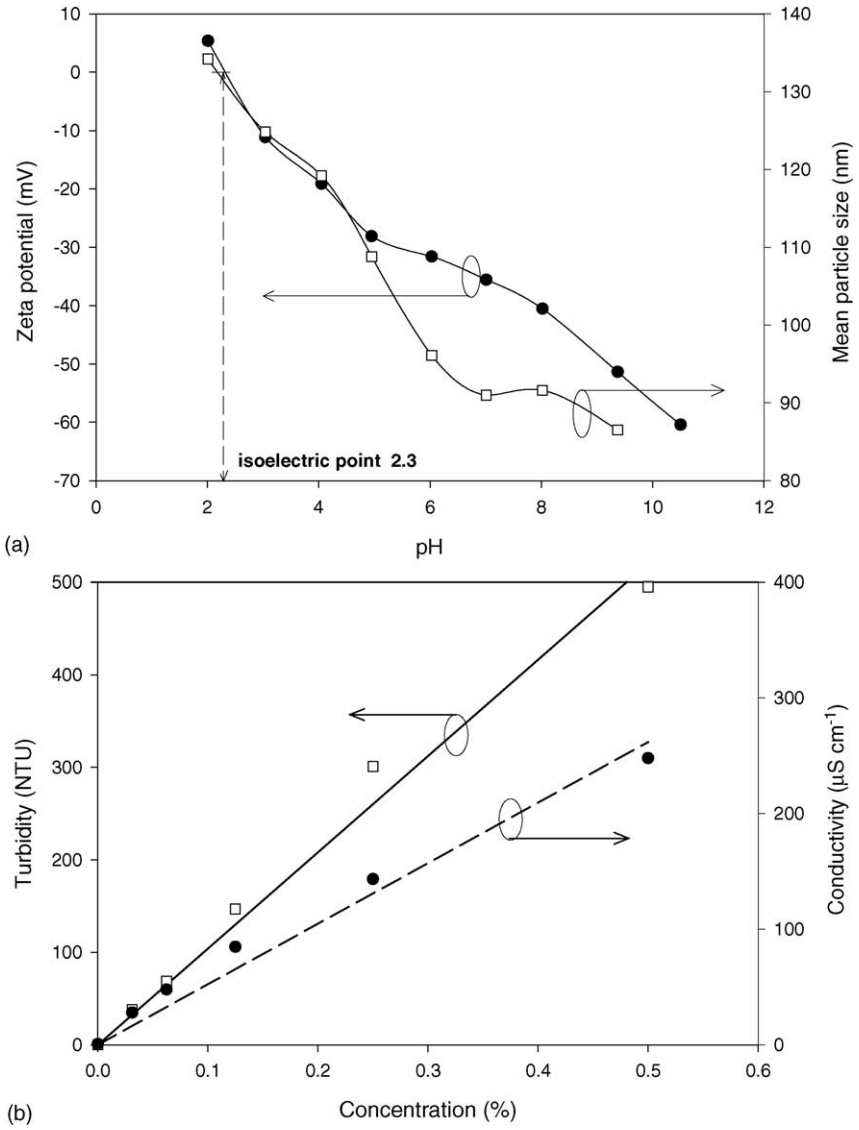

Fig. 2. (a) Variation of ζ-potential and mean particle size with wastewater pH and (b) aqueous turbidity and conductivity corresponding to the slurry dilutions (concentration) for preparation of the synthetic CMP wastewater.

kinetics, as well as the ohmic potential drop of the solution:

$$U_p = E_{eq} + \sum |\eta| + j\left(\frac{l_p}{\kappa}\right) \quad (4)$$

where l_p (m) is the inter-electrode distance, κ (mho m^{-1}) the solution conductivity, and j (A m^{-2}) represents the current density uniformly distributed over the active surface of each anode in the monopolar configuration.

Fig. 3 shows the measured cell potential as a function of the applied current density for wastewater with a range of aqueous conductivity between 60 and 250 μS cm^{-1}, along with the theoretical curves calculated from the Ohmic potential drop. It can be seen that the Ohmic potential curves substantially underestimated the actual cell voltages, especially at low κ and large j, indicating that over-potentials were significant under the operating conditions. In principal, the small differences between the Ohmic and measured voltage at very low j were mainly due to E_{eq}, and the widening gaps at higher j were mainly attributed to the j-driven over-potential as depicted by the well-known Tafel equation. Furthermore, in the electrocoagulation process with iron anodes, the precipitates of iron oxides or hydroxides were primarily gelatinous and tended to collect on the anodic surface (Fig. 1c), producing a gelatinous surface film that could also increase the anodic over-potential by passivation, particularly at large j that intensifies the surface passivation. Mass transport resistance due to concentration polarization near the anodes could also contribute to the over-potential since the system was operated with primarily laminar-flow regimes with little mixing.

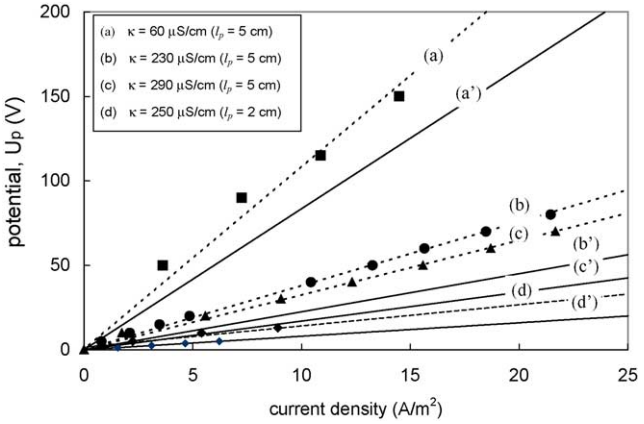

Fig. 3. Dependence of electrolysis voltage on the wastewater conductivity and applied current density (pH 9.5, temperature = 26–28 °C, flowrate = 130 mL min^{-1}). The symbols with dash-lines indicate the measured cell potential, whereas the solid lines represent the Ohmic potential drops.

3.3. Effect of charge loading for electrocoagulation

In the electrocoagulation process with iron as the anodes, the following cell reactions are expected:

$$\text{Anode}: \text{Fe}-2e^- \rightarrow \text{Fe}^{2+} \quad (5)$$

$$\text{Cathode}: 2H_2O + 2e^- \rightarrow H_{2(g)} + 2OH^- \quad (6)$$

$$\text{Overall cell}: \text{Fe} + 2H_2O \rightarrow \text{Fe}^{2+} + H_{2(g)} + 2OH^- \quad (7)$$

Theoretically, each Faraday of charge passing through a cell circuit produces 27.9 g of Fe^{2+} in the cell, and thus the reactor charge loading defined in Eq. (3) should be proportional to the quantity of ferrous ions available for electrocoagulation. Fig. 4 presents a consolidated plot showing the effect of charge loading on the steady-state turbidity removal efficiency. It can be observed that the resulting turbidity removal efficiencies clustered into a single characteristic profile, although the removal efficiency for the wastewater with low initial turbidity (70 NTU) was somewhat higher than those with higher initial turbidity (400 NTU) under similar charge loadings. The discrepancy, however, could be attributed both to the difference in the initial turbidity as well as to the difference in the wastewater conductivity. As mentioned earlier, higher suspension concentration (i.e., higher turbidity) resulted in higher aqueous conductivity, which in turn led to lower electrical field strength under the same applied current. This sequence, therefore, may potentially lower the turbidity removal efficiency. More importantly, the profile exhibited in Fig. 4 indicates that the turbidity removal efficiency increased sharply with charge loadings up to a level of approximately 8 F m^{-3}, then leveled off with larger charge loadings. Apparently, under conditions of low charge loading, the released ferrous ions were not sufficient to destabilize the silica colloids in the wastewater, limiting the removal efficiency of turbidity. Under larger values of charge loading (>8 F m^{-3}), the slowing of turbidity removal efficiency was likely controlled by the rate of particle aggregation, which is known to be a much slower process as compared to the colloidal destabilization process. From this perspective, it would also be possible to experience reduced turbidity removal efficiency under larger charge loadings, because excessive dosage of Fe^{2+} may cause restabilization of colloids by fully surrounding the silica and turning them into positively charged particles.

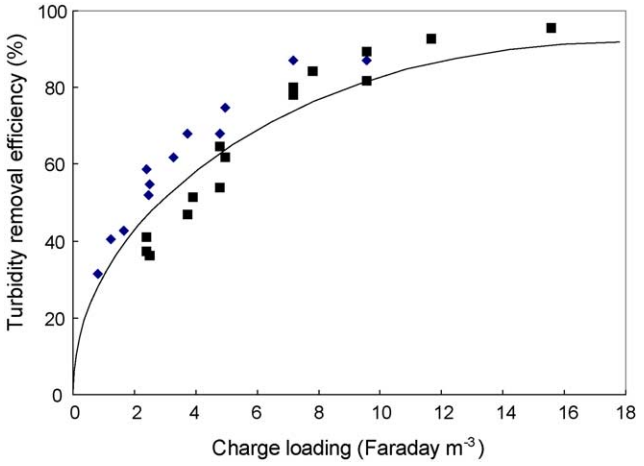

Fig. 4. Dependence of turbidity removal efficiencies on charge loading for wastewaters with low turbidity ((♦): T_0 = 70 NTU) and high turbidity ((■): T_0 = 400 NTU).

3.4. Effects of applied current density

Since charge loading is a surrogate parameter that combines contributions from the applied current and the hydraulic retention time, it would also be of interest to examine their effects on the turbidity removal as individual parameters. For this purpose, Fig. 5 presents the turbidity removal efficiency as a function of applied current density for four different hydraulic retention times. Each value of the residual turbidity was taken after the electrocoagulation process had reached

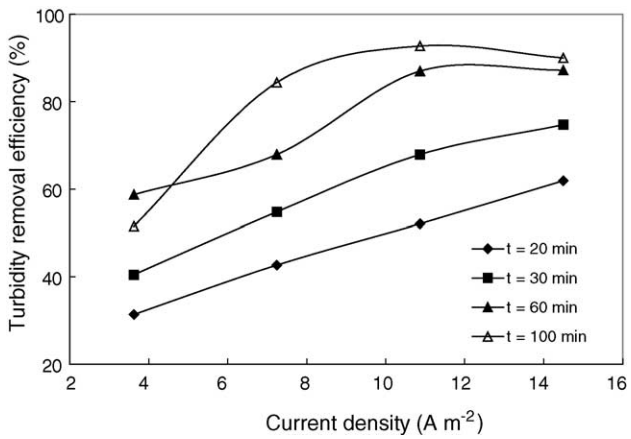

Fig. 5. Effect of applied current density on the steady-state turbidity removal efficiency at different hydraulic retention times (T_0 = 70 NTU, l_p = 5 cm).

an apparent steady-state condition, normally after 60 min of operation. As can be seen from the figure, the residual turbidity in the effluent invariably decreased with an increase in either applied current density or retention time due to the greater quantity of iron dissolution for coagulation, as well as the stronger electrical field that accelerated particle migration toward the anodes. In addition, the turbidity removal was not satisfactory (<70%) at the applied current density less than 8 A m^{-2}, unless long retention times (e.g., τ = 100 min) were allowed. More interestingly, the removal efficiencies increased almost linearly with the applied current density at the retention times of 20 and 30 min. When the retention time was prolonged to 60 and 100 min, however, the corresponding removal efficiencies tended to level off, or even decreased, at larger applied current densities. Incidentally, the quantity of residual iron concentration in the effluents also demonstrated a strong dependency on the current density, as shown in Fig. 6. At the retention time of 30 min, the residual iron concentration fluctuated between 1 and 2 mg L^{-1}, indicating that the liberated ions were effectively consumed. This result, coupled with the linear increase of the turbidity removal efficiency with current density, suggests that the process was still limited by the dosage of ferrous ion available for coagulation. For the retention times of 60 and 100 min, the residual iron concentrations were substantially less than those for the retention time of 30 min, which was consistent with the results of better removal efficiency under the same current densities for longer retention times. However, the residual iron concentration sharply increased (>7 mg L^{-1}) when the current density was raised to 10.9 A m^{-2}, then further to 14.5 A m^{-2}. Also, the fact that the profiles of residual iron concentrations were very similar for the retention times of 60 and 100 min indicates that the effect of flowrate on turbidity removal was less significant than the current density when sufficiently long retention time was allowed. The drastic increase in the residual iron concentration was also visually observed by noting the intensified yellowish color in the reactor as the current density was increased. As mentioned previously, applying higher current density would have caused restabilization of colloids, eventually leading to reduced turbidity removal efficiency as well as very high residual iron concentration.

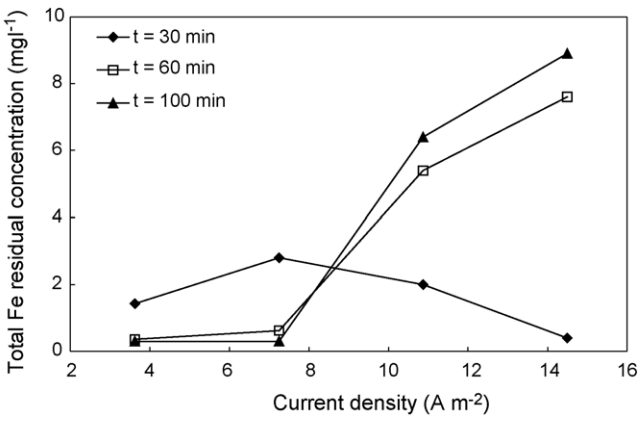

Fig. 6. The effect of current density on the residual iron concentration in the effluents for wastewater treated at various hydraulic retention times (T_0 = 70 NTU, l_p = 5 cm).

3.5. Effect of hydraulic retention time

The effect of hydraulic retention time on the colloidal removal in parallel-plate electrodes are two-fold, namely the time required for the colloidal migration due to electrophoresis toward the anodic surface, and the time required for the actual coagulation process to occur. Liberation of ferrous ions is considered instantaneous and should not be a limiting factor as compared to colloidal migration and coagulation. For the purpose of identifying the predominant effect of the flowrate, the characteristic time of particle migration was estimated and compared to that of the effective particle retention time in the active region of the electrodes. Conceptually, colloidal destabilization and aggregation mainly occur near the anodic surface because the mass transport of the liberated ions was driven by diffusion only [16]. This is also supported by the growth of gelatinous film on the anodes as well as the accumulating sediments at the foot of each anode. Consequently, the characteristic time for colloidal migration is defined as the time required for particles locating farthest from the anodes to reach the anodic surface. By performing a force balance (i.e., electrophoretic force and drag force) in the direction normal to the bulk fluid flow, a steady-state electrophoretic migration velocity can be obtained:

$$u = \frac{qE}{6\pi\mu R_p} \tag{8}$$

where E is the electrical field strength (V m^{-1}), μ the dynamic viscosity of water, R_p the mean particle radius, and q the particle charge (C) which can be calculated from a modified Debye–Hückel expression [17]:

$$q = \frac{4\pi\varepsilon R_p}{|\zeta|} \tag{9}$$

In the last equation, ζ is the measured zeta potential (−55 mV at pH 9.5), and ε is the dielectric constant of water (6.95×10^{-19} C^2 J^{-1} m^{-1} at 25 °C). Accordingly, application of current densities from 3.6 to 14.5 A m^{-2} would yield characteristic migration times between 2 and 4 s with an inter-electrode distance of 50 mm. The range of these characteristic times was more than two orders of magnitude smaller than the effective particle retention times used in this study, implying that the migration velocity under the experimental conditions was not a limiting factor to the particle removal efficiency. In contrast, the rate of actual coagulation appeared to dictate the system performance, and that the hydraulic retention time must be sufficiently long to allow coagulation process to complete. Lai and Lin [12] previously reported that, in their batch study for electrocoagulation of CMP suspension using cast iron as the electrodes (E = 375 V m^{-1}), approximately 30 min was needed for particle aggregation

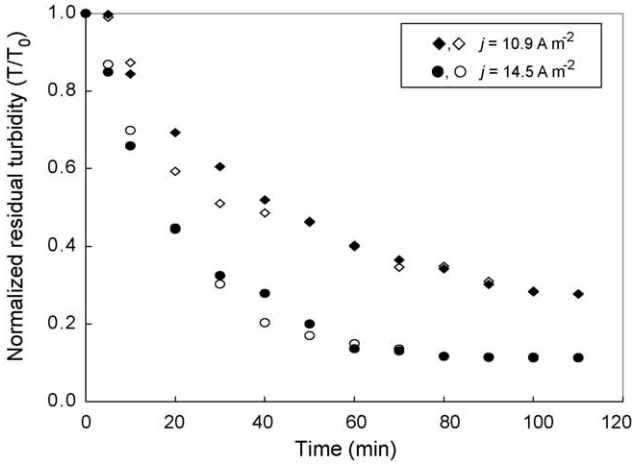

Fig. 7. Effect of inter-electrode distance (solid symbols: 5 cm, hollow symbols: 2 cm) on the turbidity removal (T_0 = 400 NTU, τ = 60 min).

to take effect and 80 min to complete. Matteson et al. [13] also estimated the coagulation time required for 50% particle reduction of kaolin suspensions (medium R_p = 1200 nm, ζ = −33 mV at pH 10.8) ranged between 50 and 100 min for applied potentials between 15 and 50 V with steel mesh as the electrodes. These ranges of coagulation time appear to concur with our experimental results, and help explain the enhanced turbidity removal efficiencies at hydraulic retention times of 60 and 100 min.

3.6. Effects of inter-electrode distance

In a parallel-plate monopolar reactor, the electrical field strength in each cell channel can be controlled by varying the applied current, but is theoretically independent of the inter-electrode distance under the same current. In order to verify whether this presumption holds true for the channelized cell reactor used in this study, the reactor was arranged such that the inter-electrode distance was positioned at either 20 mm or 50 mm apart, while the number of electrodes remained identical. Fig. 7 shows the normalized turbidity removal profile (initial turbidity of 400 NTU) using the different inter-electrode distances under two current densities (10.9 and 14.5 A m^{-2}). The results reveal improved turbidity removal at greater current density, which was attributed to the liberation of ferrous ions as mentioned earlier. However, for operation under both applied current densities, no discernable differences between the removal profiles corresponding to the two different inter-electrode distances were observed. These results demonstrate that the continuous-flow, channelized reactor indeed operates very similarly to a monopolar reactor with fully divided cells.

3.7. Process comparison between chemical and electrocoagulation

Since chemical coagulation is still considered as the primary method for treatment of CMP wastewater for majority of the chip-making facilities, it is of particular interest to compare the performance of the electrocoagulation vis-à-vis chemical coagulation. As shown in Table 2, the quality of the treated water by chemical coagulation and electrocoagulation with respect to residual turbidity was comparable, both reaching below 5 NTU when correctly treated. The electrocoagulation process, however, does not require preliminary adjustment of pH, which in itself stages a significant advantage because pH adjustment for a large quantity of wastewater is never cost-effective. Moreover, it was observed that electrocoagulation process was capable of removing organic compounds from the CMP wastewater. In this study, the removal of total organic carbon (TOC) was typically more than 60% at the charge loadings of 8 F m^{-3} for a wide range of initial wastewater TOC (5–30 mg L^{-1}). It has been documented that, in electrocoagulation, indirect oxidation via electron transfer of metal ions plays a much more important role than direct oxidation of adsorbed molecules on the anodic surface [12,18]. Nevertheless, the nature of low conductivity of the CMP wastewater may have inhibited more efficient removal of the organic components.

Table 2 also shows the jar-test results using PACl as the chemical coagulant for wastewater with different initial turbidities. From the data presented for the wastewater with low turbidity (74 NTU), it was determined that the pH must be maintained in the range between 4 and 7 to achieve particle

Table 2
Comparison of electrocoagulation with chemical coagulation processes

Process	Initial turbidity (NTU)	PACl dosage (mg L^{-1} as Al)	pH	ζ-Potential (mV)	Mean particle size (nm)	Residual turbidity[a] (NTU)	Sludge dry solid (wt.% kg m^{-3} water)
Chemical coagulation[a]	74.2	3.0	2	+11.2	90	70	0.66
			4	+2.5	2350	4.9	
			6	+5.8	3650	2.8	
			8	−10.1	200	18	
			10	−43.2	150	53	
	200	10	6.0	Not measured		1	1.96
	400	25	6.0	Not measured		3	4.43
Electrocoagulation[b]	250	–	9.5	Not measured		3	1.09

[a] Residual turbidity measured after 40 min of settling.
[b] System operated under j = 14.5 A m^{-2} and τ = 100 min for 13 h.

instability and growth in the particle size, and consequently effective turbidity removal. This result is consistent with the knowledge that the hydrolysis products such as $Al(OH)^{2+}$, $Al(OH)_2{}^{+}$, and $Al(OH)_3$ generally form from PACl under a narrow pH range between 5 and 6 [19]. The jar-test results also indicate that the minimum PACl dosage required for effective turbidity removal progressively increased with the initial wastewater turbidity, from as little as 3 mg L^{-1} (as Al) for turbidity of 70 NTU up to 25 mg L^{-1} for turbidity of 400 NTU at pH of 6. As a consequence, the dry solid weight of the sludge also increased accordingly.

To make a preliminary assessment with respect to sludge production by electrocoagulation, the system was continuously operated for more than 13 h for a wastewater turbidity of 250 NTU. The sludge was then collected by gathering the bottom sediment and by scraping as much deposited flocs off the anode surfaces as possible. As shown in Table 2, the dry solid weight of the resulting sludge from the electrocoagulation process (1.1 kg m^{-3}) was significantly less than that from PACl coagulation (>2 kg m^{-3}) for treatment of wastewater with similar initial turbidities. The low sludge volume (18 L m^{-3}) generated by iron electrocoagulation process has also been documented in other studies [12]. Although these results could only serve as preliminary assessment by discounting important sludge properties such as water content, they nevertheless provide a strong evidence that the electrocoagulation process could conceivably reduce substantial sludge volumes, especially in view of the operating difficulties for chemical coagulation that often lead to coagulant overdosing.

4. Conclusions

The performance of a continuous-flow, channelized parallel-plate electrocoagulation system for treating synthetic oxide CMP wastewater was investigated. The dilute silica slurry was representative to the actual oxide CMP wastewater, possessing a discharge pH between 9 and 10, ζ-potential more than -50 mV, and aqueous conductivity of approximately 250 μS cm^{-1} at 0.4% dilution from original silica CMP slurry, equivalent to an initial turbidity of 400 NTU. The experimental results revealed that the turbidity removal efficiency could be enhanced by increasing either the applied current or the hydraulic retention time, and that the removal efficiency was linearly correlated with the charge loading up to a level of 8 F m^{-3}. Under short hydraulic retention time ($\tau \leq 30$ min), the turbidity removal efficiency was controlled by the current density, indicating that the process was limited by the dosage of the liberated ferrous ions. For longer retention times, however, a threshold level of current density appeared to exist, and operations beyond this level would lead to process deterioration. Calculation of the characteristic migration time of particles due to electrophoresis indicated that the electrocoagulation process was not limited by the rate of particle migration, but by the rate of actual particle aggregation and coagulation that occur near the anodic surfaces. Preliminary appraisal between electro and chemical coagulation demonstrated that the former process produced lesser amount of dry sludge, and did not require pre-adjustment of wastewater pH.

Acknowledgements

This work is funded by the National Science Council (NSC) of the Republic of China through project grant NSC90-2211-317-001. The authors also wish to acknowledge the National Nano Device Laboratories (NDL) for their general supply of CMP slurries and assistance in particle size measurements.

References

[1] M.S. Kim, S.W. Woo, J.G. Park, Jpn. J. Appl. Phys. 41 (2002) 6342.
[2] B. Maag, D. Boning, B. Voelker, Semicond. Int. 23 (2000) 101.
[3] SEMATECH International, International Technology Roapmap for Semiconductors, SEMATECH, Austin, TX, 2001.
[4] J.H. Golden, R. Small, L. Pagan, C. Chang, S. Ragavan, Semicond. Int. 23 (2000) 85.
[5] J.H. Golden, J.E. Carrubba, Semicond. Fabtech. 13 (2001) 123.
[6] S. Browne, V. Krygier, J. O' Sullivan, E.L. Sandstrom, MICRO 17 (1999) 77.
[7] W. Jiang, C. Huang, H. Wu, Proceedings of the International Water Association Asia Environmental Technology Conference, Suntech City, Singapore, 30 October–1 November, 2001.
[8] R. Woodling, Semicond. Fabtech. 14 (2001) 69.
[9] G.C.C. Yang, T.-Y. Yang, S.-H. Tsai, Water Res. 37 (2003) 784.
[10] B.M. Belongia, P.D. Haworth, J.C. Baygents, S. Raghavan, J. Electrochem. Soc. 146 (1999) 4124.
[11] C. Tsouris, D.W. DePaoli, J.T. Shor, Z.-C. Hu, T.-Y. Ying, Colloids Surf. A 177 (2001) 223.
[12] C.L. Lai, S.H. Lin, Chem. Eng. J. 95 (2003) 205.
[13] M.J. Matteson, R.L. Dobson, R.W. Glenn, N.S. Kukunoor, W.H. Waits, E.J. Clayfield, Colloids Surf. A 104 (1995) 101.
[14] W. Den, C. Huang, S.-S. Chiou, Proceedings of the Ninth International Semiconductor Environmental Health and Safety Conference (ISESH), San Diego, California, 9–13 June, 2002.
[15] C. Kan, C. Huang, J.R. Pan, Colloids Surf. A 203 (2002) 1.
[16] G. Chen, X. Chen, P.L. Yue, Chem. Eng. Sci. 57 (2002) 2449.
[17] P.C. Hiemenz, R. Rajagopalan, Principles of Colloid and Surface Chemistry, third ed., Marcel Dekker, New York, 1997.
[18] J. Dziewinski, S. Marczak, E. Nuttall, G. Purdy, W. Smith, J. Taylor, C. Zhou, Waste Manage. 18 (1998) 257.
[19] R.D. Latterman, in: R.D. Latterman, A. Amirtharajah, C.R. O'Melia (Eds.), Water Quality and Treatment, McGraw-Hill, New York, 1999.